genes

Article

Genetic Mapping by 55K Single-Nucleotide Polymorphism Array Reveals Candidate Genes for Tillering Trait in Wheat Mutant *dmc*

Kemeng Jiao [1], Guojun Xia [1,2], Yuan Zhou [1], Chenyu Zhao [1], Huiyuan Yan [1], Menglei Qi [1], Pingfan Xie [1], Yongjing Ni [3], Jingxue Zhao [1], Jishan Niu [1,2], Zhaofei Chao [4], Jiangping Ren [1,2] and Lei Li [1,2,*]

1 Henan Technology Innovation Centre of Wheat/National Engineering Research Centre for Wheat, Henan Agricultural University, Zhengzhou 450046, China; j548654@163.com (K.J.); gmgs002@163.com (G.X.); zy200102242023@163.com (Y.Z.); 13782885547@163.com (C.Z.); 13523408147@163.com (H.Y.); 15639491503@163.com (M.Q.); 18530091591@163.com (P.X.); 18625453972@163.com (J.Z.); jsniu@henau.edu.cn (J.N.); xmzxrjp@126.com (J.R.)
2 National Key Laboratory of Wheat and Maize Crop Science, College of Agronomy, Henan Agricultural University, Zhengzhou 450046, China
3 Henan Engineering Research Centre of Wheat Spring Freeze Injury Identification, Shangqiu Academy of Agriculture and Forestry Sciences, Shangqiu 476000, China; nyj317@163.com
4 Jiaozuo Seed Industry Development Center, Jiaozuo 454150, China; 13903895296@139.com
* Correspondence: lilei@henau.edu.cn

Abstract: Background: The tiller number is a key agronomic trait for increasing the yield potential of wheat (*Triticum aestivum* L.). A number of quantitative trait loci (QTLs) and key genes controlling tillering have been identified, but the regulatory mechanisms remain unclear. Methods: In this study, we utilized the dwarf-monoculm mutant (*dmc*) obtained from the ethyl methane sulfonate (EMS)-treated wheat cultivar Guomai 301. The F_2 populations were constructed using the *dmc* mutant crossed to multiple tiller parents. The F_2 populations were surveyed for tillering traits at the critical fertility stage for genetic analyses. The extreme-tillering-phenotype plants from the F_2 population were used to construct mixing pools that were analyzed by a wheat 55K SNP array. The tillering genes of *dmc* were mapped using the wheat 55K SNP array combined with transcriptomic data. Results: The results showed that the genetic phenotype of *dmc* is controlled by two dominant genes. The tillering genes of *dmc* were mapped on the 60–100 Mb region of chromosome 5B and the 135–160 Mb region of chromosome 7A. A total of sixteen candidate genes associated with the tillering trait of *dmc* were identified. Two candidate genes, TraesCS5B02G058800 and TraesCS7A02G184200, were predicted to be involved in indole acetic acid (IAA) response and transport, which were considered as potential regulatory genes. Conclusions: This study elucidated the genetic basis of the *dmc* mutant and provided two valuable reference genes for studying the development and regulatory mechanisms of wheat tillering.

Keywords: *dmc*; tillering mutant; 55K SNP array; gene mapping

check for updates

Citation: Jiao, K.; Xia, G.; Zhou, Y.; Zhao, C.; Yan, H.; Qi, M.; Xie, P.; Ni, Y.; Zhao, J.; Niu, J.; et al. Genetic Mapping by 55K Single-Nucleotide Polymorphism Array Reveals Candidate Genes for Tillering Trait in Wheat Mutant *dmc*. *Genes* **2024**, *15*, 1652. https://doi.org/10.3390/genes15121652

Academic Editor: Zhuo Chen

Received: 26 November 2024
Revised: 15 December 2024
Accepted: 20 December 2024
Published: 22 December 2024

Copyright: © 2024 by the authors. Licensee MDPI, Basel, Switzerland. This article is an open access article distributed under the terms and conditions of the Creative Commons Attribution (CC BY) license (https://creativecommons.org/licenses/by/4.0/).

1. Introduction

Wheat plays a crucial role in global food security, serving as a vital food crop that feeds billions of people worldwide [1–3]. According to relevant studies, global grain trade will be affected by both climate extremes and population growth, with a reduction in wheat supply capacity in key supply regions [4–7]. Tillering is a critical aspect of plant development, particularly in grasses and cereal crops, as it significantly influences biomass production and yield [8]. Tiller formation has a significant effect on wheat in terms of building a rational population, increasing the number of effective spikes and grain yield [9,10]. Therefore, it is necessary to excavate the key genes of tiller regulation and study the mechanism of tiller formation in wheat.

The regulation of tillering involves a complex interplay of genetic factors, hormonal signaling, and environmental conditions [11–13]. The continued growth of tillers requires a steady supply of sugar. The early cessation of tillering in the *tiller inhibition mutant (tin)* mutant leads to a reduction in the number of tillers [14]. High-density planting reduces photosynthetically active radiation (PAR) intensity and causes the earlier cessation of tiller development [8]. Cytokinin (CK)-mediated signaling effects of fertilizer nitrogen forms can be employed as a management tool to regulate the tiller number in cereal crops [15]. Gibberellins (GAs) and strigolactones (SLs) are the two major phytohormones determining plant tillering, *Oryza sativa GROWTH-REGULATING FACTOR7(OsGRF7)* alters the endogenous strigolactone content, which rendered repression of the outgrowth of the axillary buds [16]. The *TILLER NUMBER 1(TN1)* gene promotes wheat tillering, at least partially, through two layers of molecular mechanisms via repressing abscisic acid (ABA) biosynthesis and inhibiting ABA signaling through preventing the binding of *PYR-like (TaPYL)* to *PROTEIN PHOSPHATASE 2C (TaPP2C)* [17]. Gibberellins also play a role in stimulating tiller development, although their effects can vary between species [18,19]. Previous correlative studies of *dmc* mutants have shown that tillering is associated with the IAA biosynthesis pathway [20]. Studying the *dmc* mutant could enhance our understanding of the complex regulatory network of tillering development.

Tillering originates from the axillary meristem (AM), and its formation and development primarily occur in two stages: (1) the development of the axillary meristem, which begins with the formation of a boundary between the shoot apex and the leaf primordia, followed by the initiation of meristematic cells in the axillary region near the leaf axil; (2) the elongation of the axillary bud, leading to the formation of tillers [21,22]. Many crops with tiller-related genes have been reported. Regulator genes in rice (*Oryza sativa* L.) influencing AM formations include *O. sativa homeobox1* (*OSH1*) [23], *LAX PANICLE1* (*LAX1*) [24], LAX PANICLE2 *(LAX2)* [25], *MONOCULM1* (*MOC1)* [26–28], *MOC1 interacting protein1 (MIP1)* [29], *Tillering and Dwarf1 (TAD1)* [30], *SLENDER RICE1 (SLR1)* [28], *MONOCULM3 (MOC3)* [31], *RICE FLORICULA/LEAFY (RFL)* [32], *Oryza sativa CUP-SHAPED COTYLEDON1 (OsCUC1)* [33], and *FRIZZLE PANICLE* (*FZP)* [34], while regulator genes influencing AM growth into tillers include *DWARF3* (*D3)* [35], *DWARF10 (D10)* [36], *DWARF14 (D14)* [37], *HIGH TILLERING DWARF1 (HTD1)* [38], *DWARF27 (D27)* [39], *O. sativa MORE AXILLARY GROWTH1a (OsMAX1a)* [40], *O. sativa MORE AXILLARY GROWTH1e (OsMAX1e*) [40], *DWARF53 (D53)* [37], *(O. sativa MINICHROMOSOME MAINTENANCE1, AGAMOUS, DEFICIENS and SERUM RESPONSE FACTOR57) (OsMADS57)* [41], *O. sativa TEOSINTE BRANCHED1 (OsTB1)* [41], *IDEAL PLANT ARCHITECTUTRE1 (IPA1)* [42], *O. sativa DENSE AND ERECT PANICLE1 (DEP1)* [42], *O. sativa SHORT INTERNODES1OsDEP1 (OsSHI1)* [42], *O. sativa CIRCADIAN CLOCK ASSOCIATED1 (OsCCA1)* [43], *Heading date 3a (Hd3a)* [44], *O. sativa Domains Rearranged Methyltransferase2* (*OsDRM2)* [45], *FLORAL ORGAN NUMBER1 (FON1*) [31], *TILLER NUMBER 1 (TN1)* [46], and *TN1 interaction factor 1 (TIF1)* [46]. Regulator genes in wheat regulating tillering include *TILLER NUMBER 1 (TN1)*, *tiller inhibition mutant (tin)*, *tin2*, *tin3*, *tin4*, *tin5*, *tin6*, *fertile tiller inhibition gene (ftin)*, and *oligo-tillering mutant (ot1)*, having diverse effects on axillary bud development and overall wheat growth [8,14,47–52].

Tillering mutants are crucial for understanding the genetic and physiological mechanisms that regulate tillering in various plant species, particularly in crops like wheat and rice. These mutants provide valuable insights into the factors that influence tiller development. Morphological studies indicate that mutants like *tin*, *tin4*, *tin5*, *ftin*, *and TN1* exhibit decreased tiller numbers due to inhibited or abnormal axillary bud development [17,47–49,53]. In *tin* mutants, tiller growth ceases when the plant transitions from the vegetative to the reproductive stage [14,54,55]. The *ftin* mutants show normal tiller numbers at the seedling stage, but exhibit a significant reduction at heading, suggesting that the reduction is due to delayed tiller outgrowth rather than inhibited axillary bud differentiation [49]. In *tin4*, *tin5*, and *TN1*, the decreased tiller number results from the inhibition of secondary tiller bud development [17,47,48]. The ot1 mutant maintained an average of three tillers [52].

Meanwhile, in *dmc*, a non-tillering mutant from EMS-treated wheat cultivar Guomai 301, both tiller bud differentiation and development are inhibited [56,57]. This means that our material, *dmc* mutants, is different from the mutants that have been reported.

In this study, we combined transcriptomic information by wheat 55K SNP array sequencing [56], and sixteen candidate genes were predicted within the two target interval segments. Two of them, TraesCS5B02G058800 and TraesCS7A02G184200, are tillering regulatory genes, which were predicted to be involved in IAA response and transport.

2. Materials and Methods

2.1. Plant Material

The dwarf-monoculm mutant *dmc* was obtained from an EMS-mutagenized population of the wheat variety Guomai 301. Through consecutive years of single-plant selection, we successfully obtained genetically stable strains of *dmc*. The hybridization of the *dmc* mutant with Aikang 58, Chinese Spring, Guomai 301, Zhengmai 379, and Zhengmai 9405 produced 15, 6, 17, 27, and 21 F_1 individuals, respectively. The F_1 individual, self-pollinated *dmc* mutant and Aikang 58, Chinese Spring, and Guomai 301 produced 460, 811, and 1041 F_2 individuals, respectively. These F_1 individuals and F_2 populations were planted in Xiaowu Village, Yuanyang City, Henan, China (35°6′ N, 113°56′ E, 70 m a.s.l.). All materials were sown in mid-October and harvested in June of the following year in 2023 and 2024 wheat growth seasons. All F_1 and F_2 individuals were sown in 2 m rows with 25 cm row spacing, leaving approximately 10 cm between plants. Varieties were obtained from the National Engineering Research Centre for Wheat. Fertilizer and weed management were similar to wheat breeding [58].

2.2. Phenotypic Investigations and Genetic Analysis

At least 30 plants of the *dmc* mutant and wheat cultivar Guomai 301 were surveyed phenotypically at the tillering stage and filling stages. A statistical analysis was conducted using Origin 2022 software. All lines of the F_2 population were surveyed for the tiller number in each April of 2023 and 2024. The data were statistically analyzed using SPSS v20 software.

2.3. Cytological Karyotype Analysis

Chromosome configurations and a high-resolution chromosome painting analysis of plants derived from the *dmc* mutant at the metaphase of mitosis: Chromosome samples were prepared as previously described [59]. For chromosome painting, eight single-strand oligonucleotides were used to form modified multiplex probes for the karyotype analysis in wheat, which included TAMRA (6-carboxytetramethylrhodamine)-modified oligonucleotides pAs1-1, pAs1-3, pAs1-4, pAs1-6, AFA-3, and AFA-4, and two FAM (6-carboxyfluorescein)-modified oligonucleotides, pSc119.2-1 and (GAA)10 [59]. Oligonucleotide probes used for FISH are listed in Table S1. The FISH procedure was tested as previously described [59]. Chromosomes were visualized with microscope Olympus BX51 (Olympus, Beijing, China) and pictures were captured with SPOT CCD (SPOT Cooled Color Digital Camera, Leica, Germany). An image analysis was conducted using Photoshop v6.0.

2.4. Wheat 55K SNP Array Analysis

Nine no-tillering and thirty multi-tillering individuals with extreme phenotypes from the Aikang58 × *dmc* F_2 populations were prepared to construct two pools. Genomic DNA was extracted by Nakayukin Marker Company (http://www.cgmb.com.cn/, accessed on 26 April 2023) (Beijing, China). The bulked samples were genotyped with the Axiom® Wheat 55K SNP array. The work was mainly conducted at Nakayukin Marker Company (http://www.cgmb.com.cn/, accessed on 26 April 2023). We performed an SNP gene analysis and cluster analysis using Biosearch's high-throughput genotyping assay platform (https://www.biosearchtech.com/, accessed on 26 April 2023). We excluded SNP markers with deletion rates greater than 20%, allele frequencies less than 5%, and those that could

not be localized to chromosomes. We screened SNP markers with differences in the mixed pools that corresponded to the extreme phenotypes. We compared and analyzed the sequences of the selected SNP markers with the Chinese Spring Genome Version 1.0 (http://www.wheatgenome.org/, accessed on 26 April 2023) for chromosome localization.

2.5. Expression Analysis

We collected tiller nodes from the *dmc* and Guomai 301 varieties separately. RNA was extracted using a Trizol reagent (TransGen Biotech, Beijing, China) according to the manufacturer's protocol. RNA concentration was measured using a NanoDrop 2000 (NanoDrop Technologies, Wilmington, DE, USA). RNA integrity was assessed using the RNA Nano 6000 Assay Kit on the Agilent Bioanalyzer 2100 system (Agilent Technologies, Santa Clara, CA, USA). We used Primer5 software to design gene-specific primers (Table S2). The wheat actin gene was used as an internal control gene. The qRT-PCR reactions were performed in 20 μL volumes containing 10 μL Hieff® qPCR SYBR Green Master Mix (Yeasen Biotech, Shanghai, China), 0.8 μL primer mix (10 μM), 1 μL cDNA (50 ng), and 8.8 μL ddH_2O. The PCR parameters were 94 °C for 30 s, and then 40 cycles of 94 °C for 5 s, and 60 °C for 30 s. All qRT-PCR reactions were replicated three times. The gene expression levels were calculated according to the $2^{-\Delta\Delta Ct}$ method [60].

3. Results

3.1. Identification of dmc Mutants

The *dmc* mutant was previously characterized from the EMS-treated wheat cultivar Guomai 301. At the tillering stage, Guomai 301 exhibited 9–12 tillers, whereas the *dmc* mutant displayed only one main stem (Figure 1A,C). At the filling stage, Guomai 301 produced approximately 20 tillers, while the *dmc* mutant developed only one main stem (Figure 1B,D). During the three-leaf stage, the *dmc* mutant presented a small tiller bud compared to the multiple tiller buds of Guomai 301 (Figure 1E).

3.2. Fluorescence In Situ Hybridization Analysis of dmc Mutant Chromosomes

To validate and identify the chromosome constitution of the *dmc* mutant, high-resolution chromosome painting was applied using eight single-strand oligonucleotide probes. The result of the fluorescence in situ hybridization analysis of chromosomes revealed that the A, B, and D genomes of the *dmc* mutant were structurally normal. There is no large segment deletions compared to the control Guomai 301 (Figure 2A,B). This finding indicates that the phenotype of the *dmc* mutant is not attributable to chromosomal structural variations.

3.3. Genetic Analysis of Tiller Number of dmc Mutant

The *dmc* mutant was crossed with several multi-tiller parents (Table 1). The F_1 generation was examined for a genetic analysis of the tiller number associated with the *dmc* mutant. The tiller count in the F_1 generation was intermediate between that of the *dmc* mutant and the multi-tiller parents. This suggests that the *dmc* mutant may be regulated by a semi-dominant gene.

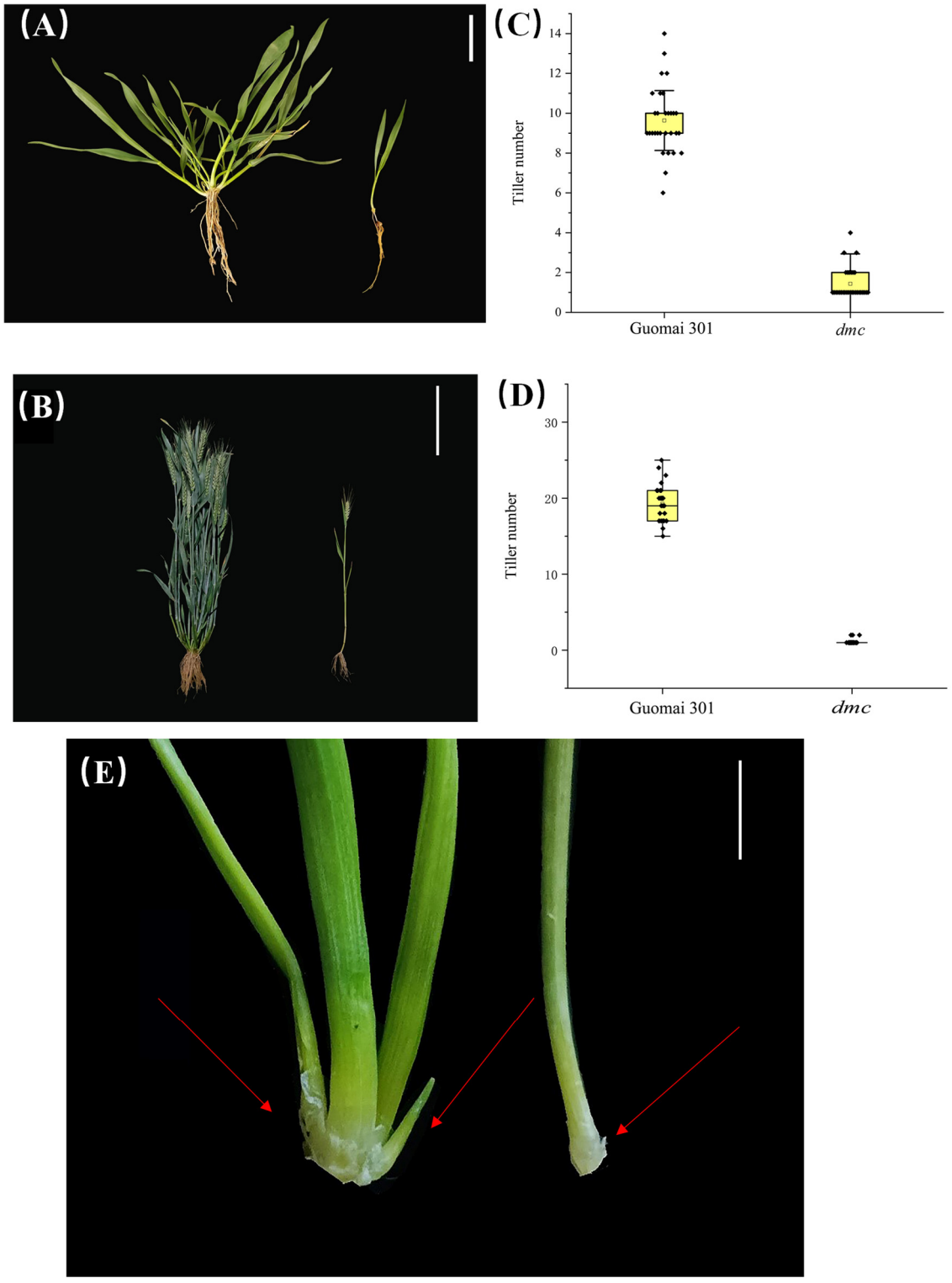


Figure 1. Phenotypes of the *dmc* mutant; (**A**) Guomai 301 (left) and the *dmc* mutant (right) at the tillering stage, and the scale bar is 5 cm; (**B**) Guomai 301 (left) and the *dmc* mutant (right) at the filling stage, and the scale bar is 10 cm; (**C**) the number of tillers at the tillering stage of Guomai 301 and the *dmc* mutant, and the data are the mean ± SD (n = 30 biologically independent samples); (**D**) the number of tillers at the filling stage of Guomai 301 and the *dmc* mutant, and the data are the mean ± SD (n = 30 biologically independent samples); (**E**) the tiller buds at the three-leaf stage of Guomai 301 (left) and the *dmc* mutant (right), the scale bar is 0.5 cm, and red arrows indicate the position of axillary buds.

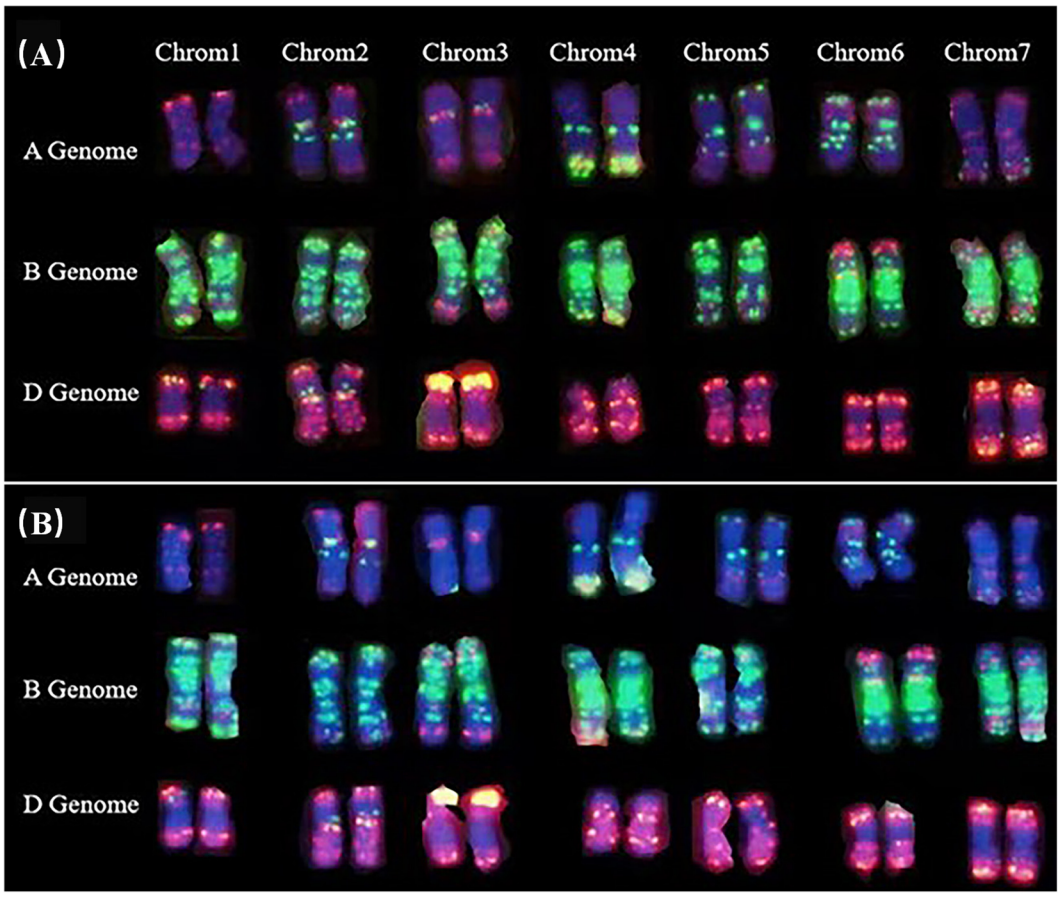


Figure 2. The high-resolution chromosome painting analysis of the plants derived from the *dmc* mutant at the metaphase of mitosis. (**A**) One karyotype of Guomai 301, which had 42 normal chromosomes. (**B**) One karyotype of the *dmc* mutant, which had 42 normal chromosomes. Blue color, chromosomes counterstained with DAPI; green, signals of oligos pSc119.2-1, (GAA)10; red, signals of oligos AFA-3, AFA-4, pAs1-1, pAs1-3, pAs1-4, and pAs1-6. Scale bar = 10 μm.

Table 1. The amount of tillering in the F_1 generation of the different hybrid combinations.

Hybrid Combination	Number of Individual F_1 Plants	Number of Tillers of Multi-Tiller Parent	Number of Tillers in the F_1 Generation [1]
dmc × Zhengmai 9405	4	13 ± 1.48	9.75 ± 5.58
Zhengmai 9405 × *dmc*	17	13 ± 1.48	4.64 ± 1.93
dmc × Aikang 58	3	22 ± 2.23	5 ± 2
Aikang 58 × *dmc*	13	22 ± 2.24	5.53 ± 1.39
dmc × Zhengmai 379	17	14 ± 1.14	8.9 ± 3.73
Zhengmai 379 × *dmc*	10	14 ± 1.14	5.23 ± 2.07
dmc × Guomai 301	11	23 ± 2.22	11.75 ± 2.06
Guomai 301 × *dmc*	6	23 ± 2.22	6.18 ± 4.52

[1] The data are the means ± SD.

The *dmc* mutant showed only one main stem but with an ineffective tiller. In the experiment, the number of effective tillers greater than one was defined as multiple tillers, and only one main stem was defined as a no-tiller plant. Assuming that the no-tiller trait is controlled by two genes, the survey showed that the F_2 populations of *dmc* × Aikang 58 in 2023, *dmc* × Chinese Spring in 2023 and 2024, and *dmc* × Guomai 301 in 2024 had 36, 27, 20, 21, and 50 no tillers, respectively (Table 2). The multiple tillers had 424, 396, 368, 380, and 385 tillers, respectively (Table 2). The result of the χ^2 test showed that the number of effective tillers was $\chi^2 < P_{0.05}$, which is consistent with the Mendelian two-gene inheritance

of a 15:1 segregation ratio. It was concluded that the no-tiller phenotype of the *dmc* mutant was controlled by two genes.

Table 2. Genetic analysis of tillering traits in F_2 populations.

Hybrid Combination	Year	Multiple Tillers	No Tiller	Expected Ratio	χ^2	*p*-Value [1]
					χ^2 (15:1)	$P\ *_{0.05}$
dmc × Aikang 58	2023	424	36	15:1	1.95	3.84
dmc × Chinese Spring	2023	396	27	15:1	0.0013	3.84
	2024	368	20	15:1	0.795	3.84
dmc × Guomai 301	2023	380	21	15:1	0.702	3.84
	2024	585	50	15:1	2.858	3.84

[1] When *df* is 1, the significance value of $P\ *_{0.05}$ is 3.84.

It shows that in the F_2 populations from the crosses of *dmc* × Chinese Spring, *dmc* × Aikang 58, and *dmc* × Guomai 301, a greater number of plants exhibited fewer tillers than those with a higher number of tillers (Figure 3). This observation supports the involvement of semi-dominant genes in the F_1 generation. We supposed that two semi-dominant genes regulate the no-tillering trait. The number of dominant genes associated with this trait varies by phenotype. For instance, the AABB genotype is characterized by the no-tillering trait.

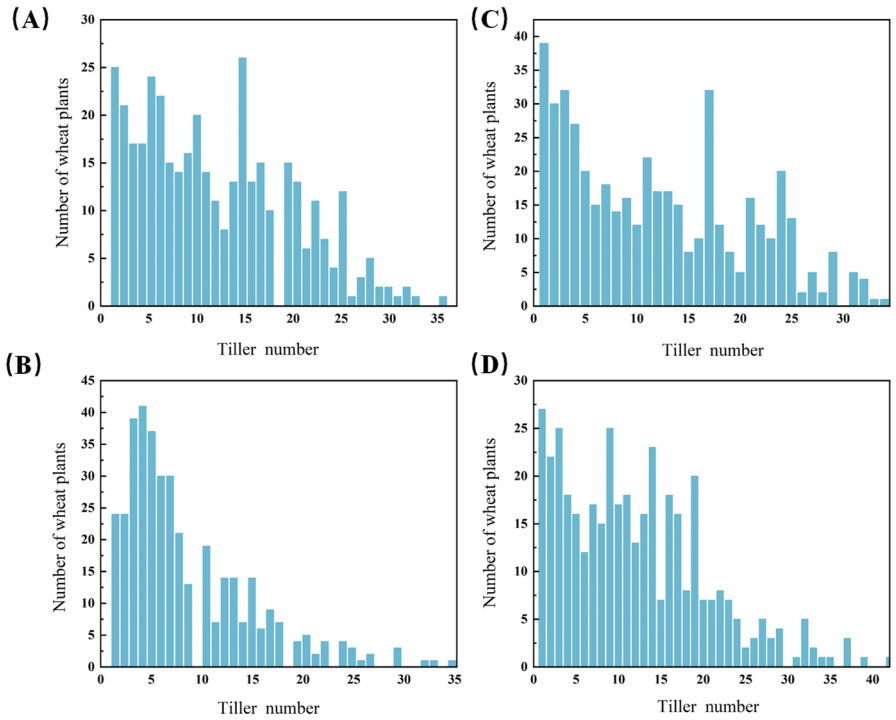


Figure 3. The effective tiller number and distribution frequency of the F_2 population; (**A**) the F_2 population of *dmc* × Guomai 301 in 2023; (**B**) the F_2 population of *dmc* × Aikang 58 in 2023; (**C**) the F_2 population of *dmc* × Chinese Spring in 2024; (**D**) the F_2 population of *dmc* × Chinese Spring in 2023.

3.4. Analysis of Gene Microarrays

An F_2 population consisting of 460 individuals derived from the cross between Aikang58 and the *dmc* mutant was used for the analysis. We first conducted a bulked segregant analysis and wheat 55K SNP array-based genotyping using the individuals with extreme phenotypes from the F_2 progenies. A total of 491 SNPs were polymorphic, of which 169 were located on chromosome 5B and 58 were located on chromosome 7A (Figure 4A).

A further analysis showed that 58 SNPs are enriched over a 60 to 100 Mb interval on the short arm of chromosome 5B, and 21 SNPs are enriched over a 135 to 160 Mb interval on the short arm of chromosome 7A (Figure 4B,C).

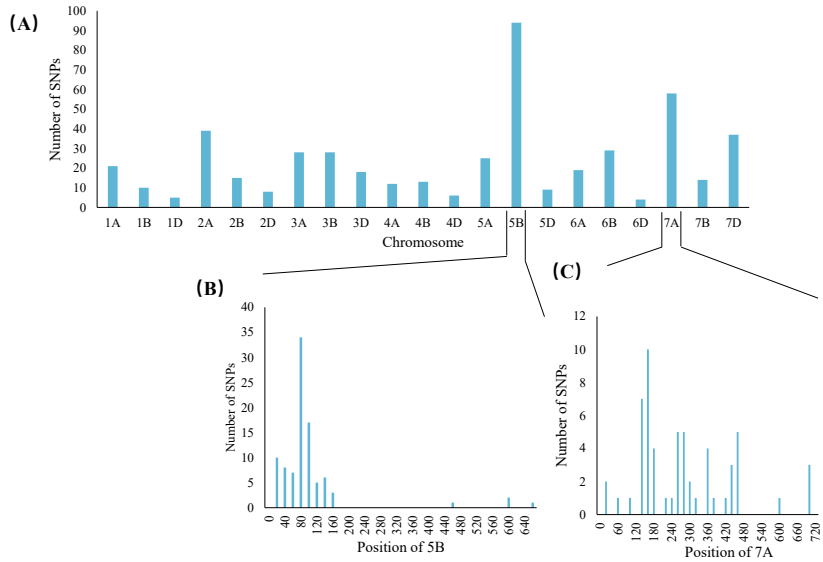


Figure 4. Distribution of single-nucleotide polymorphisms (SNPs) on different chromosomes and polymorphic SNP sites on chromosomes 5B and 7A in wheat; (**A**) number of polymorphic SNPs on each chromosome; (**B**) distribution of polymorphic SNP sites on chromosome 5B; (**C**) distribution of polymorphic SNP sites on chromosome 7A.

3.5. Candidate Gene Prediction

Combined with the transcriptome data, the differential genes contained in the two candidate intervals were analyzed and annotated [56,61]. A total of sixteen differentially expressed genes were identified (Table 3). According to transcriptome data, seven candidate genes on chromosome 5B and TraesCS7A02G184200 are upregulated in the *dmc* mutant, while the remaining eight genes on chromosome 7A are downregulated in the *dmc* mutant. The gene annotation revealed that TraesCS5B02G058800 is involved in regulating growth hormone response proteins. And TraesCS7A02G184200 encodes a protein featuring the BTB structural domain, which plays a role in the transport of growth hormones. This finding aligns with our previous studies where IAA metabolism and signaling affected tillering development of the *dmc* mutant [20]. Consequently, TraesCS5B02G058800 and TraesCS7A02G184200 are two potential candidate genes regulating tillering development for further research.

Table 3. Gene annotation of differentially expressed genes in candidate intervals on 5B and 7A.

#	Gene	Annotation	Expression in *dmc*
1	TraesCS5B02G058800	Auxin-responsive protein IAA31	up
2	TraesCS5B02G059300	CBL-interacting protein kinase 4	up
3	TraesCS5B02G059800	Tuliposide A-converting enzyme 2, chloroplastic	up
4	TraesCS5B02G060200	Dolabradiene monooxygenase	up
5	TraesCS5B02G060300	Dolabradiene monooxygenase	up
6	TraesCS5B02G061600	11-beta-hydroxysteroid dehydrogenase A	up
7	TraesCS5B02G062500	Methylcrotonoyl-CoA carboxylase subunit alpha	up
8	TraesCS7A02G184200	Protein containing a Bric-a-Brac/Tramtrack/Broad (BTB) complex and an NPH3 domain (BTBN), regulation of auxin transport	down
9	TraesCS7A02G184600	Shikimate kinase domain-containing protein	up
10	TraesCS7A02G187800	Aquaporin NIP III subfamily protein	down

Table 3. *Cont.*

#	Gene	Annotation	Expression in *dmc*
11	TraesCS7A02G188100	Amino acid transporter	down
12	TraesCS7A02G188400	Plant regulator RWP-RK domain-containing protein	down
13	TraesCS7A02G191400	Small GTP-binding protein OsRac3	down
14	TraesCS7A02G191700	Domain of unknown function DUF23	down
15	TraesCS7A02G196100	TGF-beta receptor, type I/II extracellular region family protein	down
16	TraesCS7A02G197900	Similar to CEL5=CELLULASE 5 (fragment)	down

We performed a qRT-PCR analysis of sixteen candidate genes' expression during the tillering stage of Guomai 301 and *dmc* for the validation of transcriptome data (Figure 5). It showed that the qRT-PCR results matched well with the transcriptome data.

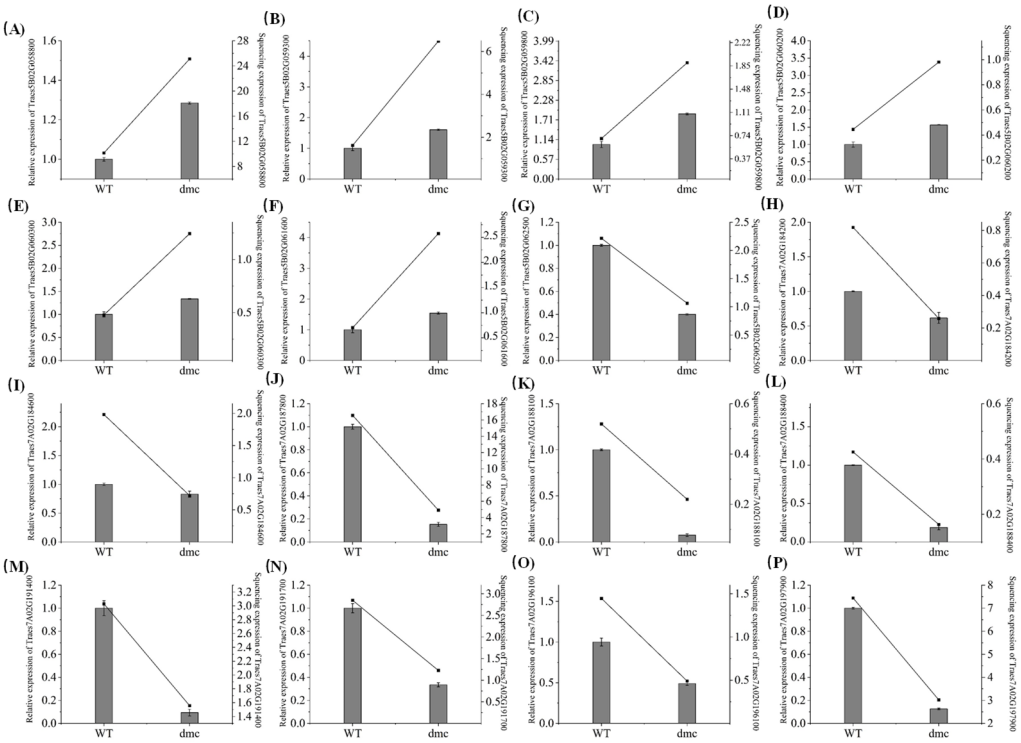


Figure 5. The qRT-PCR analysis of sixteen candidate genes. (**A**) TraesCS5B02G058800 (Auxin-responsive protein IAA31); (**B**) TraesCS5B02G059300 (CBL-interacting protein kinase 4); (**C**) TraesCS5B02G059800 (Tuliposide A-converting enzyme 2); (**D**) TraesCS5B02G060200 (Dolabradiene monooxygenase); (**E**) TraesCS5B02G060300 (Dolabradiene monooxygenase); (**F**) TraesCS5B02G061600 (11-beta-hydroxysteroid dehydrogenase A); (**G**) TraesCS5B02G062500 (Methylcrotonoyl-CoA carboxylase subunit alpha); (**H**) TraesCS7A02G184200 (Protein containing a BTB complex and an NPH3 domain (BTBN), regulation of auxin transport); (**I**) TraesCS7A02G184600 (Shikimate kinase domain-containing protein); (**J**) TraesCS7A02G187800 (Aquaporin NIP III subfamily protein); (**K**) TraesCS7A02G188100 (Amino acid transporter); (**L**) TraesCS7A02G188400 (Plant regulator RWP-RK domain-containing protein); (**M**) TraesCS7A02G191400 (Small GTP-binding protein OsRac3); (**N**) TraesCS7A02G191700 (Domain of unknown function DUF23); (**O**) TraesCS7A02G196100 (TGF-beta receptor, type I/II extracellular region family protein); (**P**) TraesCS7A02G197900 (Similar to CEL5 = CELLULASE 5). The left y-axis represents relative expression, and relative expressions are shown by histograms. The right y-axis represents the expression value (FPKM) of transcriptome sequencing, and expression values are shown by lines. Error bars indicate the standard deviation. The x-axis indicates the samples of Guomai 301 and *dmc*.

4. Discussion

Increasing wheat yield is an important means to cope with future food shortages [62–64]. It is an effective way to increase wheat yield to study the mechanism of tillering control and increase the amount of effective tillering [47,65]. In the *dmc* mutant, the growth of tiller buds and plant development are inhibited (Figure 1A,B). Most of the primordia could not grow or stopped developing, which resulted in no tillers [56].The *dmc* mutant exhibits a dwarf phenotype with no tillers, making it an excellent material for studying tiller suppression.

Previous studies have reported eight tillering inhibition genes of wheat (*tin1*, *tin2*, *tin3*, *ftin*, *TIN4*, *TIN5*, *tin6*, *TN1)* [8,14,17,47–51]. Among these, the natural mutants *tin*, *tin2*, *ftin*, and *TIN4* are located on 1AS, 2A, 1AS, and 2DL, respectively [8,14,47,49]. The EMS-treated mutants *tin3*, *TIN5*, *tin6*, and *TN1* are located on chromosomes 3A, Tu7, 2DL, and 6BS, respectively [8,17,48,50,51]. The QTL associated with the tiller number in wheat is located on chromosomes 1A, 1B, 2B, 2D, 4A, 4B, 4D, 5A, 6B, and 7D [66–72]. In this study, we predicted two new wheat tiller inhibition genes, whose physical locations are different from those of *pin-formed 1* (*TaPIN1)* [73], *dwarf (TaD27-B)* [39], *ovarian tumor domain-containing proteases 1 (TaOTUB1)* [74], and *squamosa promoter binding-like 14* (*TaSPL14)* [75] found previously on chromosomes 5B and 7A. This study contains a new finding of a tillering inhibition mutant (Figure 4B,C).

The downregulated gene expressions related to phytohormone syntheses of auxin, zeatin, cytokinin, and some transcription factor (TF) families of TALE, and WOX, might be the major causes of non-tillering in mutant *dmc* [20,56,57,76]. The gene *tin* reduces tillering by controlling the early maturation of internodes, causing a competition for sucrose between the internodes and tiller buds [14,53]. Similarly, *TN1* inhibits tillering by regulating the levels of ABA [17]. The *ot1* gene revealed the upregulation of genes associated with SL and ABA biosynthesis and signaling [52]. Previous studies have proved that IAA contents in *dmc* were significantly less than that in Guomai 301 at tillering stages [56]. In this study, TraesCS5B02G058800 and TraesCS7A02G184200 are related to IAA regulation and transport among the sixteen candidate genes identified in the positional cloning prediction. We predict that they are candidate genes of non-tillering in the *dmc* mutant (Table 3).

Using homologous gene cloning methods, several genes related to wheat tillering have been identified [77,78]. These genes act at different developmental stages of wheat growth and participate in the regulation of tillering through interactions with various genetic factors or exogenous hormones. For instance, *MOC1* encodes a putative GRAS family nuclear protein that is expressed mainly in the axillary buds and functions to initiate axillary buds and to promote wheat outgrowth [28]. In contrast, the *TaTB1* gene overexpression in wheat results in reduced tillers and spike numbers [79]. Additionally, *phytochrome-interacting factor-like 1* (*TaPIL1)* activates the transcriptional expression of wheat *TaTB1*, reducing the wheat tiller number [80]. Moreover, *the PLANT ARCHITECTURE AND YIELD 1 (TaPAY1)* gene could improve the tiller number via affecting polar IAA transport activity and altering endogenous IAA distribution [81]. The *TaPIN1s* indicating that IAA might mediate the axillary bud production and reduction in *TaPIN1* expression increased the tiller number and grain yield per plant of wheat [73,82,83]. The application of SL inhibits shoot branching in plants [84]. The *TaD27-B* modulates tillering by participating in the biosynthesis of SL, while *TaD53* acts as a repressor in the SL signaling pathway, interacting with the transcriptional co-repressor Topless (*TaTPL)* [39]. The *TERMINAL FLOWER 1 (TaTFL1)* was implicated in tiller regulation by IAA and CK signaling [85]. These examples illustrate the complexity of factors regulating wheat tillering. However, only the mechanisms of ABA and SL in tiller regulation have been reported, while the role of IAA in this process remains unclear. Our previous studies have shown that IAA expression in *dmc* is suppressed, which is a critical factor causing the dwarfing and no tillering in this mutant [20,56]. Therefore, *dmc* provides a valuable new mutant material for studying the mechanisms of tillering in wheat, holding significant implications for molecular breeding in the crop.

5. Conclusions

In this study, F_1 individuals and F_2 populations of the *dmc* mutant obtained by multi-tillering varieties were constructed for a genetic analysis and oligotillering gene mapping. The populations showed that the genetic phenotype of the *dmc* mutant was controlled by two dominant genes. The analysis of a wheat 55K SNP array showed that the *dmc* tiller gene was located on the 60–100 MB region of chromosome 5B and the 135–160 MB region of chromosome 7A. A total of sixteen candidate genes related to *dmc* tillering traits were identified in the candidate region by combining the wheat 55K SNP array results with the transcriptome information of *dmc* mutants. Among them, TraesCS5B02G058800 and TraesCS7A02G184200 genes are predicted to be involved in the response and transport of IAA, and are considered as potential regulatory genes of tillering. Cloning the *dmc* tillering gene could aid in developing tillering-related markers for wheat breeding and enhance our understanding of the biological mechanisms underlying this complex trait.

Supplementary Materials: The following supporting information can be downloaded at: https://www.mdpi.com/article/10.3390/genes15121652/s1, Table S1: Oligonucleotide probes used for FISH; Table S2: Primers used in the experiment and their sequence information.

Author Contributions: K.J. performed all the experiments pertaining to trait observation, photograph taking, and qRT-PCR and also analyzed the data and drafted the manuscript. Y.Z., C.Z., H.Y., G.X. and Z.C. helped with sowing and sample preparation. M.Q. and P.X. helped with sowing, trait observation, and figure drawing. Y.N. and J.Z. contributed to sowing and the data analysis. J.R., J.N. and L.L. helped with writing—review and editing. L.L. designed the whole study, and contributed to conceptualization, project administration. All authors have read and agreed to the published version of the manuscript.

Funding: This research was supported by the National Key R&D Program of China (Program No. 2023YFD2301500, No. 2017YFD0301101), the National Natural Science Foundation of China (NSFC, 32171972), the Project of Zhongyuan Scholars Workstation (224400510001), and the Key Research Project of the Shennong Laboratory (SN01-2022-01).

Institutional Review Board Statement: Not applicable.

Informed Consent Statement: Not applicable.

Data Availability Statement: The original contributions presented in this study are included in the article. Further inquiries can be directed to the corresponding author.

Conflicts of Interest: The authors declare no conflicts of interest.

References

1. Luo, X.M.; Yang, Y.M.; Lin, X.L.; Xiao, J. Deciphering spike architecture formation towards yield improvement in wheat. *J. Genet. Genom.* **2023**, *50*, 835–845. [CrossRef] [PubMed]
2. Sareen, S.; Dadrasi, A.; Chaichi, M.; Nehbandani, A.; Sheikhi, A.; Salmani, F.; Nemati, A. Addressing food insecurity: An exploration of wheat production expansion. *PLoS ONE* **2023**, *18*, e0290684.
3. Luo, L. Is strigolactone signaling a key player in regulating tiller formation in response to nitrogen? *Front. Plant Sci.* **2022**, *13*, 1081740. [CrossRef] [PubMed]
4. Almeshal, A.M.; Almazrouee, A.I.; Alenizi, M.R.; Alhajeri, S.N. Forecasting the spread of COVID-19 in Kuwait using compartmental and logistic regression model. *Appl. Sci.* **2020**, *10*, 3402. [CrossRef]
5. Sun, H.W.; Ma, J.H.; Wang, L. Changes in per capita wheat production in China in the context of climate change and population growth. *Food Secur.* **2023**, *15*, 597–612. [CrossRef]
6. Dadrasi, A.; Chaichi, M.; Nehbandani, A.; Soltani, E.; Nemati, A.; Salmani, F.; Heydari, M.; Yousefi, A.R. Global insight into understanding wheat yield and production through Agro-Ecological Zoning. *Sci. Rep.* **2023**, *13*, 15898. [CrossRef]
7. Yang, B.; Qiao, L.; Zheng, X.; Zheng, J.; Wu, B.; Li, X.; Zhao, J. Quantitative Trait Loci Mapping of Heading Date in Wheat under Phosphorus Stress Conditions. *Genes* **2024**, *15*, 1150. [CrossRef]
8. Shang, Q.S.; Wang, Y.P.; Tang, H.; Sui, N.; Zhang, X.S.; Wang, F. Genetic, hormonal, and environmental control of tillering in wheat. *Crop J.* **2021**, *9*, 986–991. [CrossRef]
9. Beveridge, C.A.; Rameau, C.; Wijerathna-Yapa, A.; Lunn, J. Lessons from a century of apical dominance research. *J. Exp. Bot.* **2023**, *74*, 3903–3922. [CrossRef]

10. Schneider, A.; Godin, C.; Boudon, F.; Demotes-Mainard, S.; Sakr, S.; Bertheloot, J. Light Regulation of Axillary Bud Outgrowth Along Plant Axes: An Overview of the Roles of Sugars and Hormones. *Front. Plant Sci.* **2019**, *10*, 1296. [CrossRef]
11. Zhu, M.Q.; Jiang, S.; Huang, J.Q.; Li, Z.H.; Xu, S.; Liu, S.J.; He, Y.G.; Zhang, Z.H. Biochemical and Transcriptome Analyses Reveal a Stronger Capacity for Photosynthate Accumulation in Low-Tillering Rice Varieties. *Int. J. Mol. Sci.* **2024**, *25*, 1648. [CrossRef] [PubMed]
12. Lyu, J.; Huang, L.Y.; Zhang, S.L.; Zhang, Y.S.; He, W.M.; Zeng, P.; Zeng, Y.; Huang, G.F.; Zhang, J.; Ning, M.; et al. Neo-functionalization of a Teosinte branched 1 homologue mediates adaptations of upland rice. *Nat. Commun.* **2020**, *11*, 725. [CrossRef] [PubMed]
13. Zhou, B.Y.; Luo, Q.; Shen, Y.H.; Wei, L.; Song, X.; Liao, H.Q.; Ni, L.; Shen, T.; Du, X.L.; Han, J.Y.; et al. Coordinated regulation of vegetative phase change by brassinosteroids and the age pathway in *Arabidopsis*. *Nat. Commun.* **2023**, *14*, 2608. [CrossRef] [PubMed]
14. Kebrom, T.H.; Richards, R.A. Physiological perspectives of reduced tillering and stunting in the tiller inhibition (*tin*) mutant of wheat. *Funct. Plant Biol.* **2013**, *40*, 977–985. [CrossRef] [PubMed]
15. Bauer, B.; von Wirén, N. Modulating tiller formation in cereal crops by the signalling function of fertilizer nitrogen forms. *Sci. Rep.* **2020**, *10*, 20504. [CrossRef]
16. Chen, Y.P.; Dan, Z.W.; Li, S.Q. Rice GROWTH-REGULATING FACTOR 7 controls tiller number by regulating strigolactone synthesis. *Plant Signal Behav.* **2020**, *15*, 1804685. [CrossRef]
17. Dong, C.H.; Zhang, L.C.; Zhang, Q.; Yang, Y.; Li, D.; Xie, Z.; Cui, G.; Chen, Y.; Wu, L.; Li, Z.; et al. Tiller Number1 encodes an ankyrin repeat protein that controls tillering in bread wheat. *Nat. Commun.* **2023**, *14*, 836. [CrossRef]
18. Li, L.; Xie, C.M.; Zong, J.Q.; Guo, H.L.; Li, D.D.; Liu, J.X. Physiological and Comparative Transcriptome Analyses of the High-Tillering Mutant mtn1 Reveal Regulatory Mechanisms in the Tillering of Centipedegrass (*Eremochloa ophiuroides* (Munro) Hack.). *Int. J. Mol. Sci.* **2022**, *23*, 11580. [CrossRef]
19. Feng, G.Y.; Xu, X.H.; Liu, W.W.; Hao, F.X.; Yang, Z.F.; Nie, G.; Huang, L.K.; Peng, Y.; Bushman, S.; He, W.; et al. Transcriptome Profiling Provides Insights into the Early Development of Tiller Buds in High- and Low-Tillering Orchardgrass Genotypes. *Int. J. Mol. Sci.* **2023**, *24*, 16370. [CrossRef]
20. Zhang, J.; Li, J.; Ni, Y.; Jiang, Y.; Jiao, Z.; Li, H.; Wang, T.; Zhang, P.; Han, M.; Li, L.; et al. Key wheat GRF genes constraining wheat tillering of mutant *dmc*. *PeerJ* **2021**, *9*, e11235. [CrossRef]
21. Luo, Z.W.; Janssen, B.J.; Snowden, K.C. The molecular and genetic regulation of shoot branching. *Plant Physiol.* **2021**, *187*, 1033–1044. [CrossRef] [PubMed]
22. Yang, Q.Q.; Yuan, C.Q.; Cong, T.C.; Zhang, Q.X. The Secrets of Meristems Initiation: Axillary Meristem Initiation and Floral Meristem Initiation. *Plants* **2023**, *12*, 1879. [CrossRef] [PubMed]
23. Tanaka, W.; Tsuda, K.; Hirano, H. Class I KNOX Gene OSH1 is Indispensable for Axillary Meristem Development in Rice. *Cytologia* **2019**, *84*, 343–346. [CrossRef]
24. Mach, J. Rice Axillary Meristem Formation Requires Directional Movement of LAX PANICLE1 Protein. *Plant Cell* **2009**, *21*, 1027. [CrossRef]
25. Tabuchi, H.; Zhang, Y.; Hattori, S.; Omae, M.; Shimizu-Sato, S.; Oikawa, T.; Qian, Q.; Nishimura, M.; Kitano, H.; Xie, H.; et al. LAX PANICLE2 of Rice Encodes a Novel Nuclear Protein and Regulates the Formation of Axillary Meristems. *Plant Cell* **2011**, *23*, 3276–3287. [CrossRef]
26. Li, X.Y.; Qian, Q.; Fu, Z.M.; Wang, Y.H.; Xiong, G.S.; Zeng, D.L.; Wang, X.Q.; Liu, X.F.; Teng, S.; Hiroshi, F.; et al. Control of tillering in rice. *Nature* **2003**, *422*, 618–621. [CrossRef]
27. Zhang, B.; Liu, X.; Xu, W.N.; Chang, J.Z.; Li, A.; Mao, X.G.; Zhang, X.Y.; Jing, R.L. Novel function of a putative MOC1 ortholog associated with spikelet number per spike in common wheat. *Sci. Rep.-UK* **2015**, *5*, 12211. [CrossRef]
28. Liao, Z.G.; Yu, H.; Duan, J.B.; Yuan, K.; Yu, C.J.; Meng, X.B.; Kou, L.Q.; Chen, M.J.; Jing, Y.H.; Liu, G.F.; et al. SLR1 inhibits MOC1 degradation to coordinate tiller number and plant height in rice. *Nat. Commun.* **2019**, *10*, 2738. [CrossRef]
29. Sun, F.L.; Zhang, W.P.; Xiong, G.S.; Yan, M.X.; Qian, Q.; Li, J.Y.; Wang, Y.H. Identification and functional analysis of the MOC1 interacting protein 1. *J. Gene Genom.* **2010**, *37*, 69–77. [CrossRef]
30. Xu, C.; Wang, Y.G.; Yu, Y.C.; Duan, J.B.; Liao, Z.G.; Xiong, G.S.; Meng, X.B.; Liu, G.F.; Qian, Q.; Li, J.Y. Degradation of MONOCULM 1 by APC/C^{TAD1} regulates rice tillering. *Nat. Commun.* **2012**, *3*, 750. [CrossRef]
31. Shao, G.N.; Lu, Z.F.; Xiong, J.S.; Wang, B.; Jing, Y.H.; Meng, X.B.; Liu, G.F.; Ma, H.Y.; Liang, Y.; Chen, F.; et al. Tiller Bud Formation Regulators MOC1 and MOC3 Cooperatively Promote Tiller Bud Outgrowth by Activating FON1 Expression in Rice. *Mol. Plant* **2019**, *12*, 1090–1102. [CrossRef] [PubMed]
32. Deshpande, G.M.; Ramakrishna, K.; Chongloi, G.L.; Vijayraghavan, U. Functions for rice RFL in vegetative axillary meristem specification and outgrowth. *J. Exp. Bot.* **2015**, *66*, 2773–2784. [CrossRef] [PubMed]
33. Wang, J.; Bao, J.L.; Zhou, B.B.; Li, M.; Li, X.Z.; Jin, J. The osa-miR164 target OsCUC1 functions redundantly with OsCUC3 in controlling rice meristem/organ boundary specification. *New Phytol.* **2020**, *229*, 1566–1581. [CrossRef] [PubMed]
34. Bai, X.F.; Huang, Y.; Hu, Y.; Liu, H.Y.; Zhang, B.; Smaczniak, C.; Hu, G.; Han, Z.M.; Xing, Y.Z. Duplication of an upstream silencer of FZP increases grain yield in rice. *Nat. Plants* **2017**, *3*, 885–893. [CrossRef] [PubMed]
35. Varshney, K.; Gutjahr, C. KAI2 Can Do: Karrikin Receptor Function in Plant Development and Response to Abiotic and Biotic Factors. *Plant Cell Physiol.* **2023**, *64*, 984–995. [CrossRef]

36. Wang, Y.X.; Shang, L.G.; Yu, H.; Zeng, L.J.; Hu, J.; Ni, S.; Rao, Y.C.; Li, S.F.; Chu, J.F.; Meng, X.B.; et al. A Strigolactone Biosynthesis Gene Contributed to the Green Revolution in Rice. *Mol. Plant* **2020**, *13*, 923–932. [CrossRef]
37. Zhou, F.; Lin, Q.B.; Zhu, L.H.; Ren, Y.L.; Zhou, K.N.; Shabek, N.; Wu, F.Q.; Mao, H.B.; Dong, W.; Gan, L.; et al. D14–SCF^{D3}-dependent degradation of D53 regulates strigolactone signalling. *Nature* **2013**, *504*, 406–410. [CrossRef]
38. Lin, H.; Wang, R.X.; Qian, Q.; Yan, M.X.; Meng, X.B.; Fu, Z.M.; Yan, C.Y.; Jiang, B.; Su, Z.; Li, J.Y.; et al. DWARF27, an Iron-Containing Protein Required for the Biosynthesis of Strigolactones, Regulates Rice Tiller Bud Outgrowth. *Plant Cell* **2009**, *21*, 1512–1525. [CrossRef]
39. Zhao, B.; Wu, T.T.; Ma, S.S.; Jiang, D.J.; Bie, X.M.; Sui, N.; Zhang, X.S.; Wang, F. *TaD27-B* gene controls the tiller number in hexaploid wheat. *Plant Biotechnol. J.* **2020**, *18*, 513–525. [CrossRef]
40. Wang, L.; Wang, B.; Jiang, L.; Liu, X.; Li, X.L.; Lu, Z.F.; Meng, X.B.; Wang, Y.H.; Smith, S.M.; Li, J.Y. Strigolactone Signaling in Arabidopsis Regulates Shoot Development by Targeting D53-Like SMXL Repressor Proteins for Ubiquitination and Degradation. *Plant Cell* **2015**, *27*, 3128–3142. [CrossRef]
41. Chen, L.P.; Zhao, Y.; Xu, S.J.; Zhang, Z.Y.; Xu, Y.Y.; Zhang, J.Y.; Chong, K. OsMADS57 together with OsTB1 coordinates transcription of its target *OsWRKY94* and *D14* to switch its organogenesis to defense for cold adaptation in rice. *New Phytol.* **2018**, *218*, 219–231. [CrossRef] [PubMed]
42. Duan, E.; Wang, Y.H.; Li, X.H.; Lin, Q.B.; Zhang, T.; Wang, Y.P.; Zhou, C.L.; Zhang, H.; Jiang, L.; Wang, J.L.; et al. OsSHI1 Regulates Plant Architecture Through Modulating the Transcriptional Activity of IPA1 in Rice. *Plant Cell* **2019**, *31*, 1026–1042. [CrossRef] [PubMed]
43. Wang, F.; Han, T.W.; Song, Q.X.; Ye, W.X.; Song, X.G.; Chu, J.F.; Li, J.Y.; Chen, Z.J. The Rice Circadian Clock Regulates Tiller Growth and Panicle Development Through Strigolactone Signaling and Sugar Sensing. *Plant Cell* **2020**, *32*, 3124–3138. [CrossRef] [PubMed]
44. Tsuji, H.; Tachibana, C.; Tamaki, S.; Taoka, K.; Kyozuka, J.; Shimamoto, K. Hd3a promotes lateral branching in rice. *Plant J.* **2015**, *82*, 256–266. [CrossRef] [PubMed]
45. Moritoh, S.; Eun, C.; Ono, A.; Asao, H.; Okano, Y.; Yamaguchi, K.; Shimatani, Z.; Koizumi, A.; Terada, R. Targeted disruption of an orthologue of DOMAINS REARRANGED METHYLASE 2, OsDRM2, impairs the growth of rice plants by abnormal DNA methylation. *Plant J.* **2012**, *71*, 85–98. [CrossRef]
46. Zhang, Q.; Xie, J.Y.; Zhu, X.Y.; Ma, X.Q.; Yang, T.; Khan, N.U.; Zhang, S.Y.; Liu, M.S.; Li, L.; Liang, Y.T.; et al. Natural variation in Tiller Number 1 affects its interaction with TIF1 to regulate tillering in rice. *Plant Biotechnol. J.* **2023**, *21*, 1044–1057. [CrossRef]
47. Wang, Z.Q.; Wu, F.K.; Chen, X.D.; Zhou, W.L.; Shi, H.R.; Lin, Y.; Hou, S.; Yu, S.F.; Zhou, H.; Li, C.X.; et al. Fine mapping of the tiller inhibition gene *TIN4* contributing to ideal plant architecture in common wheat. *Theor. Appl. Genet.* **2022**, *135*, 527–535. [CrossRef]
48. Si, Y.; Lu, Q.; Tian, S.; Niu, J.; Cui, M.; Liu, X.; Gao, Q.; Shi, X.; Ling, H.; Zheng, S. Fine mapping of the tiller inhibition gene *TIN5* in Triticum urartu. *Theor. Appl. Genet.* **2022**, *135*, 2665–2673. [CrossRef]
49. Zhang, J.P.; Wu, J.; Liu, W.H.; Lu, X.; Yang, X.M.; Gao, A.N.; Li, X.Q.; Lu, Y.Q.; Li, L.H. Genetic mapping of a fertile tiller inhibition gene, *ftin*, in wheat. *Mol. Breed.* **2012**, *31*, 441–449. [CrossRef]
50. Schoen, A.; Yadav, I.; Wu, S.Y.; Poland, J.; Rawat, N.; Tiwari, V. Identification and high-resolution mapping of a novel tiller number gene (*tin6*) by combining forward genetics screen and MutMap approach in bread wheat. *Funct. Integr. Genom.* **2023**, *23*, 157. [CrossRef]
51. Kuraparthy, V.; Sood, S.; Dhaliwal, H.S.; Chhuneja, P.; Gill, B.S. Identification and mapping of a tiller inhibition gene (*tin3*) in wheat. *Theor. Appl. Genet.* **2007**, *114*, 285–294. [CrossRef] [PubMed]
52. Bai, J.X.; Guo, H.J.; Xiong, H.C.; Xie, Y.D.; Gu, J.Y.; Zhao, L.S.; Zhao, S.R.; Ding, Y.P.; Liu, L.X. Strigolactone and abscisic acid synthesis and signaling pathways are enhanced in the wheat oligo-tillering mutant *ot1*. *Mol. Breed.* **2024**, *44*, 12. [CrossRef] [PubMed]
53. Richards, R.A. A tiller inhibitor gene in wheat and its effect on plant growth. *Crop Pasture Sci.* **1988**, *39*, 749–757. [CrossRef]
54. Kebrom, T.H.; Chandler, P.M.; Swain, S.M.; King, R.W.; Richards, R.A.; Spielmeyer, W. Inhibition of tiller bud outgrowth in the *tin* mutant of wheat is associated with precocious internode development. *Plant Physiol.* **2012**, *160*, 308–318. [CrossRef]
55. Spielmeyer, W.; Richards, R.A. Comparative mapping of wheat chromosome 1AS which contains the tiller inhibition gene (tin) with rice chromosome 5S. *Theor. Appl. Genet.* **2004**, *109*, 1303–1310. [CrossRef]
56. He, R.S.; Ni, Y.J.; Li, J.C.; Jiao, Z.X.; Zhu, X.X.; Jiang, Y.M.; Li, Q.Y.; Niu, J.S. Quantitative Changes in the Transcription of Phytohormone-Related Genes: Some Transcription Factors Are Major Causes of the Wheat Mutant *dmc* Not Tillering. *Int. J. Mol. Sci.* **2018**, *19*, 1324. [CrossRef]
57. An, J.H.; Niu, H.; Ni, Y.J.; Jiang, Y.M.; Zheng, Y.X.; He, R.S.; Li, J.C.; Jiao, Z.X.; Zhang, J.; Li, H.J.; et al. The miRNA-mRNA Networks Involving Abnormal Energy and Hormone Metabolisms Restrict Tillering in a Wheat Mutant *dmc*. *Int. J. Mol. Sci.* **2019**, *20*, 4586. [CrossRef]
58. Li, Q.Y.; Qin, Z.; Jiang, Y.M.; Shen, C.C.; Duan, Z.B.; Niu, J.S. Screening wheat genotypes for resistance to black point and the effects of diseased kernels on seed germination. *J. Plant Dis. Prot.* **2014**, *121*, 79–88. [CrossRef]
59. Du, P.; Zhuang, L.F.; Wang, Y.Z.; Yuan, L.; Wang, Q.; Wang, D.R.; Dawadondup; Tan, L.J.; Shen, J.; Xu, H.B.; et al. Development of oligonucleotides and multiplex probes for quick and accurate identification of wheat and Thinopyrum bessarabicum chromosomes. *Genome* **2017**, *60*, 93–103. [CrossRef]

60. Livak, K.J.; Schmittgen, T.D. Analysis of relative gene expression data using real-time quantitative PCR and the 2(-Delta Delta C(T)) Method. *Methods* **2001**, *25*, 402–408. [CrossRef]
61. Li, J.C.; Jiao, Z.X.; He, R.S.; Sun, Y.L.; Xu, Q.Q.; Zhang, J.; Jiang, Y.M.; Li, Q.Y.; Niu, J.S. Gene Expression Profiles and microRNA Regulation Networks in Tiller Primordia, Stem Tips, and Young Spikes of Wheat Guomai 301. *Genes* **2019**, *10*, 686. [CrossRef] [PubMed]
62. Hickey, L.T.; Hafeez, A.N.; Robinson, H.; Jackson Scott, A.; Leal-Bertioli Soraya, C.M.; Tester, M.; Gao, C.X.; Godwin Ian, D.; Hayes Ben, J.; Wulff Brande, B.H. Breeding crops to feed 10 billion. *Nat. Biotechnol.* **2019**, *37*, 744–754. [CrossRef] [PubMed]
63. Watson, A.; Ghosh, S.; Williams, M.J.; Cuddy, W.S.; Simmonds, J.; Rey, M.-D.; Hatta, M.A.M.; Hinchliffe, A.; Steed, A.; Reynolds, D.; et al. Speed breeding is a powerful tool to accelerate crop research and breeding. *Nat. Plants* **2018**, *4*, 23–29. [CrossRef]
64. Yu, H.; Li, J.Y. Breeding future crops to feed the world through de novo domestication. *Nat. Commun.* **2022**, *13*, 23–29. [CrossRef]
65. Wolde, G.M.; Mascher, M.; Schnurbusch, T. Genetic modification of spikelet arrangement in wheat increases grain number without significantly affecting grain weight. *Mol. Genet. Genom.* **2018**, *294*, 457–468. [CrossRef]
66. Liu, J.J.; Luo, W.; Qin, N.N.; Ding, P.Y.; Zhang, H.; Yang, C.C.; Mu, Y.; Tang, H.P.; Liu, Y.X.; Li, W.; et al. A 55 K SNP array-based genetic map and its utilization in QTL mapping for productive tiller number in common wheat. *Theor. Appl. Genet.* **2018**, *131*, 2439–2450. [CrossRef]
67. Wang, Z.Q.; Liu, Y.X.; Shi, H.R.; Mo, H.J.; Wu, F.K.; Lin, Y.; Gao, S.; Wang, J.R.; Wei, Y.M.; Liu, C.J.; et al. Identification and validation of novel low-tiller number QTL in common wheat. *Theor. Appl. Genet.* **2016**, *129*, 603–612. [CrossRef]
68. Naruoka, Y.; Talbert, L.E.; Lanning, S.P.; Blake, N.K.; Martin, J.M.; Sherman, J.D. Identification of quantitative trait loci for productive tiller number and its relationship to agronomic traits in spring wheat. *Theor. Appl. Genet.* **2011**, *123*, 1043–1053. [CrossRef]
69. Kato, K.; Miura, H.; Sawada, S. Mapping QTLs controlling grain yield and its components on chromosome 5A of wheat. *Theor. Appl. Genet.* **2000**, *101*, 1114–1121. [CrossRef]
70. Hu, Y.S.; Ren, T.H.; Li, Z.; Tang, Y.Z.; Ren, Z.L.; Yan, B.J. Molecular mapping and genetic analysis of a QTL controlling spike formation rate and tiller number in wheat. *Gene* **2017**, *634*, 15–21. [CrossRef]
71. Liu, J.J.; Tang, H.P.; Qu, X.R.; Liu, H.; Li, C.; Tu, Y.; Li, S.Q.; Habib, A.; Mu, Y.; Dai, S.F.; et al. A novel, major, and validated QTL for the effective tiller number located on chromosome arm 1BL in bread wheat. *Plant Mol. Biol.* **2020**, *104*, 173–185. [CrossRef] [PubMed]
72. Ren, T.H.; Hu, Y.S.; Tang, Y.Z.; Li, C.S.; Yan, B.J.; Ren, Z.L.; Tan, F.Q.; Tang, Z.X.; Fu, S.L.; Li, Z. Utilization of a Wheat55K SNP Array for Mapping of Major QTL for Temporal Expression of the Tiller Number. *Front. Plant Sci.* **2018**, *9*, 333. [CrossRef] [PubMed]
73. Yao, F.; Li, X.; Wang, H.; Song, Y.N.; Li, Z.Q.; Li, X.G.; Gao, X.Q.; Zhang, X.S.; Bie, X.M. Down-expression of *TaPIN1*s Increases the Tiller Number and Grain Yield in Wheat. *Bmc Plant Biol.* **2021**, *21*, 443. [CrossRef] [PubMed]
74. Jiang, D.; Hao, X.; Zhang, J.; Tang, H.; Wang, F. Reducing expression of *TaOTUB1*s decreases tiller number in wheat. *Plant Signal Behav.* **2021**, *16*, 201–217. [CrossRef]
75. Jian, C.; Pan, Y.; Liu, S.; Guo, M.; Huang, Y.; Cao, L.; Zhang, W.; Yan, L.; Zhang, X.; Hou, J.; et al. The TaGW2-TaSPL14 module regulates the trade-off between tiller number and grain weight in wheat. *J. Integr. Plant Biol.* **2024**, *66*, 1953–1965. [CrossRef]
76. Li, J.C.; Jiang, Y.M.; Zhang, J.; Ni, Y.J.; Jiao, Z.X.; Li, H.J.; Wang, T.; Zhang, P.P.; Guo, W.L.; Li, L.; et al. Key auxin response factor (ARF) genes constraining wheat tillering of mutant *dmc*. *PeerJ* **2021**, *9*, e12221. [CrossRef]
77. Zhao, L.; Tan, L.B.; Zhu, Z.F.; Xiao, L.T.; Xie, D.X.; Sun, C.Q. *PAY1* improves plant architecture and enhances grain yield in rice. *Plant J.* **2015**, *83*, 528–536. [CrossRef]
78. Gallavotti, A. The role of auxin in shaping shoot architecture. *J. Exp. Bot.* **2013**, *64*, 2593–2608. [CrossRef]
79. Liu, J.; Cheng, X.L.; Liu, P.; Sun, J.Q. *miR*156-Targeted SBP-Box Transcription Factors Interact with DWARF53 to Regulate *TEOSINTE BRANCHED1* and *BARREN STALK1* Expression in Bread Wheat. *Plant Physiol.* **2017**, *174*, 1931–1948. [CrossRef]
80. Zhang, L.C.; He, G.H.; Li, Y.P.; Yang, Z.Y.; Liu, T.Q.; Xie, X.Z.; Kong, X.Y.; Sun, J.Q. Transcription factors PILs directly interact with SPLs and repress tillering/branching in plants. *New Phytol.* **2021**, *233*, 1414–1425. [CrossRef]
81. Liu, R.Z. *Creation of Tillcring Germplasm Using TaPAY1 Gene in Wheat*; Shandong Agriculture University: Tai'an, China, 2021.
82. Friml, J.; Benková, E.; Blilou, I.; Wisniewska, J.; Hamann, T.; Ljung, K.; Woody, S.; Sandberg, G.; Scheres, B.; GerJürgens, G.; et al. AtPIN4 Mediates Sink-Driven Auxin Gradients and Root Patterning in *Arabidopsis*. *Cell* **2002**, *108*, 661–673. [CrossRef] [PubMed]
83. Bilanovičová, V.; Rýdza, N.; Koczka, L.; Hess, M.; Feraru, E.; Friml, J.; Nodzyński, T. The Hydrophilic Loop of Arabidopsis PIN1 Auxin Efflux Carrier Harbors Hallmarks of an Intrinsically Disordered Protein. *Int. J. Mol. Sci.* **2022**, *23*, 6352. [CrossRef] [PubMed]
84. Mikihisa, U.; Atsushi, H.; Satoko, Y.; Kohki, A.; Tomotsugu, A.; Takeda-Kamiya, N.; Magome, H.; Kamiya, Y.; Shirasu, K.; Yoneyama, K.; et al. Inhibition of shoot branching by new terpenoid plant hormones. *Nature* **2008**, *455*, 195–200.
85. Sun, J.; Bie, X.M.; Chu, X.L.; Wang, N.; Zhang, X.S.; Gao, X.Q. Genome-edited *TaTFL1-5* mutation decreases tiller and spikelet numbers in common wheat. *Front. Plant Sci.* **2023**, *14*, 1142779. [CrossRef]

Disclaimer/Publisher's Note: The statements, opinions and data contained in all publications are solely those of the individual author(s) and contributor(s) and not of MDPI and/or the editor(s). MDPI and/or the editor(s) disclaim responsibility for any injury to people or property resulting from any ideas, methods, instructions or products referred to in the content.